

# Nuclear Shapes in the Interacting Vector Boson Model

**H.G. Ganev**

Joint Institute for Nuclear Research, 141980 Dubna, Russia

**Abstract.** Nuclear shapes are investigated within the framework of the two-fluid Interacting Vector Boson Model (IVBM). The latter possesses a rich algebraic structure of physically interesting subgroups that define its distinct exactly solvable dynamical limits. Their classical images are obtained by means of the coherent state method using a variation without and with angular momentum projection. The results obtained show that the angular momentum projection turns out to be crucial for obtaining stable triaxial shapes within the framework of the IVBM in its  $SU^*(3)$  limit without breaking the exact dynamical symmetry.

## 1 Introduction

Nuclear shapes and phase transitions between them are the subject of great interest in the last years, both from experimental and theoretical points of view (see e.g. [1]). The introduction of the concept of critical point symmetry [2] has recalled the attention of the community to the topic of quantum phase transitions in nuclei. Different models have been used to study nuclear shapes and quantum phase transitions in different many-body systems, such as atomic nuclei [3], molecules [4], [5], atomic clusters [6], and finite polymers. Among these models, those based upon algebraic Hamiltonians play an important role. A nice feature of the algebraic models is the occurrence of phases connected to specific geometric configurations of the ground state, which arise from the occurrence of different dynamical symmetries. Thus, different shapes or phases in algebraic models are related to all possible breakings of the dynamical symmetry group.

The phase structure of the Interacting Vector Boson Model (IVBM) [7] has been investigated in Ref. [8]. There different shapes corresponding to its various dynamical limits have been obtained and quantum phase transitions between them analyzed. In [9] a new dynamical symmetry, based on the  $SU^*(3)$  algebra, has been introduced for the description of triaxial nuclei. It was shown that the addition of two-body perturbation terms (e.g. Majorana interaction, an  $O(6)$  term) to the  $SU^*(3)$  Hamiltonian produces stable triaxial minima, giving rise to the triaxial shapes [9].

In the present paper we reinvestigate the nuclear shapes that might appear in the IVBM phase diagram from a slightly different perspective with the emphases of obtaining triaxial shapes. For this purpose we study the nuclear shapes

appearing in the IVBM using a variational procedure without and with angular momentum projection. We show that the usage of a more accurate angular momentum projection variational procedure changes the topology of the corresponding potential energy surface in the  $SU^*(3)$  limit, giving rise to stable triaxial shapes obtained in the present approach without breaking the exact dynamical symmetry of the model.

## 2 The Model

It was suggested by Bargmann and Moshinsky [10], [11] that two types of bosons are needed for the description of nuclear dynamics. It was shown there that the consideration of only two-body system consisting of two different interacting vector particles will suffice to give a complete description of  $N$  three-dimensional oscillators with a quadrupole-quadrupole interaction. The latter can be considered as the underlying basis in the algebraic construction of the *phenomenological* IVBM [7].

The algebraic structure of the IVBM is realized in terms of creation and annihilation operators of two kinds of vector bosons  $u_m^\dagger(\alpha)$ ,  $u_m(\alpha)$  ( $m = 0, \pm 1$ ), which differ in an additional quantum number  $\alpha = \pm 1/2$  (or  $\alpha = p$  and  $n$ )—the projection of the  $T$ -spin (an analogue to the  $F$ -spin of IBM-2 or the  $I$ -spin of the particle-hole IBM).

All bilinear combinations of the creation and annihilation operators of the two vector bosons generate the boson representations of the non-compact symplectic group  $Sp(12, R)$ :

$$F_M^L(\alpha, \beta) = \sum_{k,m} C_{1k1m}^{LM} u_k^+(\alpha) u_m^+(\beta), \quad (1)$$

$$G_M^L(\alpha, \beta) = \sum_{k,m} C_{1k1m}^{LM} u_k(\alpha) u_m(\beta), \quad (2)$$

$$A_M^L(\alpha, \beta) = \sum_{k,m} C_{1k1m}^{LM} u_k^+(\alpha) u_m(\beta), \quad (3)$$

where  $C_{1k1m}^{LM}$ , which are the usual Clebsch-Gordan coefficients for  $L = 0, 1, 2$  and  $M = -L, -L + 1, \dots, L$ , define the transformation properties of (1),(2) and (3) under rotations.

Symplectic dynamical symmetries allow the change of the number of bosons, elementary excitations or phonons  $N$ , providing for richer subalgebraic structures and larger representation spaces to accommodate more structural effects. Dynamical symmetry group  $Sp(12, R)$  contains both compact and non-compact substructures, defined by different reduction chains [12]. Each chain will correspond possibly to different shape.

## 3 The IVBM Coherent States

There are many approaches which allow the association of a certain geometry to any abstract algebra, but for algebraic models, this can be achieved with the

## Nuclear Shapes in the IVBM

theory of the coherent (or intrinsic) states. The expectation value of the Hamiltonian in the ground coherent state is referred to as its classical limit.

The standard approach to obtain the geometrical properties of the system is to express the collective variables in the intrinsic (body-fixed) frame of reference. We use the following IVBM coherent states

$$|N; r_1, r_2, \theta\rangle = \frac{1}{\sqrt{N!}} (B^\dagger)^N |0\rangle \quad (4)$$

with

$$B^\dagger = \frac{1}{\sqrt{r_1^2 + r_2^2}} [r_1 p_z^\dagger + r_2 (n_x^\dagger \sin\theta + n_z^\dagger \cos\theta)]. \quad (5)$$

The geometric properties of the ground states of nuclei within the framework of the IVBM can then be studied by considering the energy functional

$$E(N; r_1, r_2, \theta) = \frac{\langle N; r_1, r_2, \theta | H | N; r_1, r_2, \theta \rangle}{\langle N; r_1, r_2, \theta | N; r_1, r_2, \theta \rangle}. \quad (6)$$

By minimizing  $E(N; r_1, r_2, \theta)$  (6) with respect to  $r_1$ ,  $r_2$ , and  $\theta$ ,  $\partial E/\partial r_1 = \partial E/\partial r_2 = \partial E/\partial \theta = 0$ , one obtains the equilibrium "shape" corresponding to any boson Hamiltonian,  $H$ . It is convenient to introduce a new dynamical variable  $\rho = r_2/r_1$  which together with the parameter  $\theta$  determine the corresponding "shape".

## 4 Nuclear Shapes

In the present section the classical limits of the model Hamiltonians representing different dynamical symmetries of the IVBM are given.

### 4.1 The $U_p(3) \otimes U_n(3)$ limit

We consider the Hamiltonian that is linear combination of first order Casimirs of  $U_\tau(3)$  ( $\tau = p, n$ ):

$$H_I = \varepsilon_p N_p + \varepsilon_n N_n. \quad (7)$$

The Hamiltonian (7) can be rewritten in the form

$$H_I = \varepsilon_p N + \varepsilon N_n, \quad (8)$$

where  $\varepsilon = \varepsilon_n - \varepsilon_p$ . The first term in (8) can be dropped since it does not contribute to the energy surface. Thus, the Hamiltonian determining the properties of the system in the  $U_p(3) \otimes U_n(3)$  limit is just

$$H_I = \varepsilon N_n. \quad (9)$$

The expectation value of (9) with respect to (4) gives the energy surface

$$E(N; \rho) = \varepsilon \frac{N \rho^2}{1 + \rho^2}. \quad (10)$$

The scaled energy  $\varepsilon(\rho) = E(N; \rho)/\varepsilon N$  in the  $U_p(3) \otimes U_n(3)$  limit is given in Figure 1. From the latter we see that the minimum is at  $\rho_0 = 0$  and is  $\theta$ -independent. This is the vibrational limit of the model and corresponds to the case of two uncoupled oscillators. The inclusion of higher-order terms in  $N_p$  and  $N_n$  will give rise to an anharmonicity.

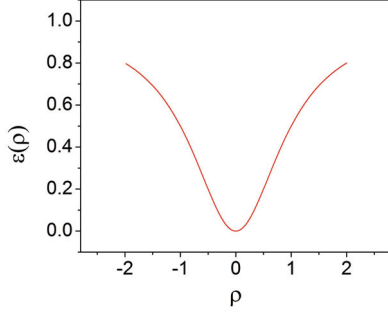


Figure 1. The scaled energy surface  $\varepsilon(\rho)$  in the  $U_p(3) \otimes U_n(3)$  limit.

#### 4.2 The $O(6)$ limit

The Hamiltonian describing the  $O(6)$  (or  $\gamma$ -unstable) properties can be written down through the  $O(6)$  pairing operator  $P^\dagger = \frac{1}{2}(p^\dagger \cdot p^\dagger - n^\dagger \cdot n^\dagger)$  in the following form

$$H_{II} = \frac{4k'}{N-1} P^\dagger P. \quad (11)$$

In (11) the  $P^\dagger P$  operator is used instead of the quadratic Casimir operator  $C_2[O(6)]$  of  $O(6)$  because of their linear dependence, i.e.  $C_2[O(6)] = -4P^\dagger P + N(N+4)$ .

Taking the expectation value of (11) one obtains the energy surface

$$E(N; \rho) = k' N \left[ \frac{1 - \rho^2}{1 + \rho^2} \right]^2, \quad (12)$$

which does not depend on  $\theta$  ( $\theta$ -unstable) and has a minimum at  $\rho_0 \neq 0$  ( $|\rho_0| = 1$ ). It corresponds to a deformed "γ-unstable" (in IBM terms) rotor.

We want to point out that actually there are two  $O_\pm(6)$  algebras, given in Ref. [8], that are isomorphic and have the same eigenspectrum but differ through phases in the wave functions resulting into different energy surfaces. The energy surface (12) corresponds to the  $O_-(6)$  limit. The other,  $O_+(6)$ , limit is not physically important since its energy surface is just a constant. The scaled energy surface  $\varepsilon(\rho)$  in the  $O_-(6)$  limit is given in Figure 2.

## Nuclear Shapes in the IVBM

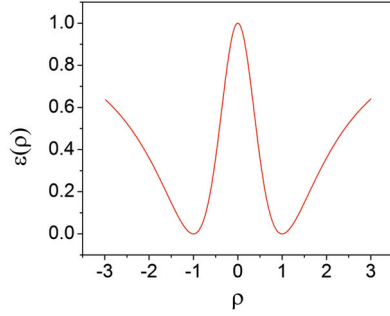


Figure 2. The scaled energy surface  $\varepsilon(\rho)$  in the  $O(6)$  limit.

### 4.3 $SU(3)$ limit

In this case we study the Hamiltonian

$$H_{III} = -\frac{k}{N-1} Q \cdot Q, \quad (13)$$

where the operator  $Q = Q_p + Q_n$  is the quadrupole generator of  $SU(3)$  of the combined two-fluid system. The operators  $Q_p$  and  $Q_n$  are defined through the operators (3) as  $Q_p = \sqrt{6}A_M^2(p, p)$  and  $Q_n = \sqrt{6}A_M^2(n, n)$ , respectively. The expectation value of (13) with respect to (4) gives

$$E(N; \rho, \theta) = -kN \frac{2}{3} \left[ \frac{1 + \rho^4 + \frac{1}{2}\rho^2(3\cos 2\theta + 1)}{(1 + \rho^2)^2} + 1 \right]. \quad (14)$$

In Figure 3 we plot the scaled energy surface  $\varepsilon(\rho, \theta) = E(N; \rho, \theta)/kN$  in the  $SU(3)$  limit.

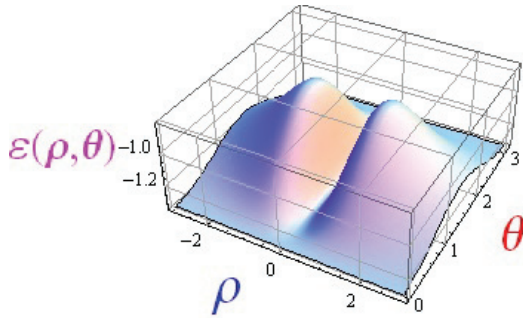


Figure 3. The scaled energy surface  $\varepsilon(\rho, \theta) = E(N; \rho, \theta)/kN$  in the  $SU(3)$  limit.

In order to see to what geometry corresponds the energy surface obtained in this case, we need the relation of the two IVBM parameters  $\rho$  and  $\theta$  with the

commonly used parameters  $\beta$  and  $\gamma$  of the geometrical collective model. In the CS of the IVBM, the effective  $\gamma_{eff}$  deformation can be defined in the usual way as [13]:

$$\tan \gamma_{eff} = \sqrt{2} \frac{\langle Q_2 \rangle}{\langle Q_0 \rangle}, \quad (15)$$

where  $\langle Q_\mu \rangle$  denotes the expectation value of the  $\mu$ th component of the quadrupole operator  $Q$ . The result is

$$\tan \gamma_{eff} = \sqrt{3} \frac{\rho^2 \sin^2 \theta}{2 + \frac{\rho^2}{2} (3 \cos 2\theta + 1)}. \quad (16)$$

From Figure 3 we see that the minimum is at  $\rho_0 = 0$ , which corresponds to  $\gamma_{eff} = 0^0$ . Taking into account the definition of  $\rho$ , we see that the ground state boson condensate (4) takes the form

$$| N; \rho = 0 \rangle = \frac{1}{\sqrt{N!}} (p_z^\dagger)^N | 0 \rangle. \quad (17)$$

Then the effective  $\beta$  deformation parameter will be proportional to the expectation value of the intrinsic quadrupole moment  $Q_0(p)$  of the  $p$ -system:

$$\beta_{eff} \simeq \langle Q_0(p) \rangle = \frac{2}{\sqrt{6}} > 0. \quad (18)$$

The values  $\gamma_{eff} = 0^0$  and  $\beta_{eff} > 0$  correspond to a prolate shape. Geometrically this corresponds to an axially deformed rotor.

#### 4.4 $SU^*(3)$ limit

This limit is appropriate for the case when the one type of particles of the two-component system is particle-like and the other is hole-like.

The  $SU^*(3)$  dynamical symmetry can be studied through the Hamiltonian

$$H_{IV} = -\frac{k'}{N-1} Q \cdot Q, \quad (19)$$

where  $Q = Q_p - Q_n$  [9]. The energy surface corresponding to it is given by

$$E(N; \rho, \theta) = -k' N \frac{2}{3} \left[ \frac{1 + \rho^4 - \frac{1}{2} \rho^2 (3 \cos 2\theta + 1)}{(1 + \rho^2)^2} + 1 \right], \quad (20)$$

and is shown in Figure 4. Similarly, one concludes that the energy surface of the  $SU^*(3)$  limit is also associated with a prolate shape ( $\beta_{eff} > 0$ ,  $\gamma_{eff} = 0^0$ ). Thus, geometrically this limit also corresponds to an axially deformed rotor.

It turns out that the addition of two-body perturbation terms (e.g. Majorana interaction, an  $O(6)$  term) to the model  $SU^*(3)$  Hamiltonian (19) produces

## Nuclear Shapes in the IVBM

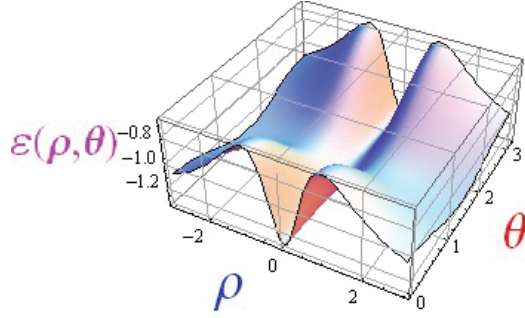


Figure 4. The scaled energy surface  $\varepsilon(\rho, \theta) = E(N; \rho, \theta)/k'N$  in the  $SU^*(3)$  limit.

stable triaxial minima, giving rise to the triaxial shapes [9]. Recall that stable triaxial shapes are obtained in the framework of IBM by adding higher-order terms to the model Hamiltonian [14], [15] or by the introduction of  $g$ -boson [16], [17] ( $sdg$ -IBM with the  $U(15)$  dynamical symmetry group). Triaxial shapes are obtained also in the IBM-2 with  $U(6) \otimes U(6)$  algebraic structure where the analysis of the nuclear shapes and the quantum phase transitions between them involve more control and order parameters [1], [18], [19], [20].

Finally, we want to point out that that we can obtain oblate equilibrium shapes in the two  $SU(3)$  and  $SU^*(3)$  limits simply by exchanging the  $x$  and  $z$  axes, which were actually considered in Refs. [8], [9].

### 5 Angular Momentum Projected Energy Surfaces

It is well known that the intrinsic state defined by Eq.(4) does not have good angular momentum. So a more accurate procedure will be first to project a condensate wave function with a good angular momentum and then to perform the variation.

The projected ground state energy which should then be minimized is [21], [22]:

$$E_{pr}(N; \rho, \theta) = \frac{\langle N; \rho, \theta | H P_{00}^{L=0} | N; \rho, \theta \rangle}{\langle N; \rho, \theta | P_{00}^{L=0} | N; \rho, \theta \rangle}, \quad (21)$$

where the projection operator is [21], [23]:

$$P_{MK}^L = \frac{2L+1}{8\pi^2} \int D_{MK}^{L*} R(\Omega) d\Omega. \quad (22)$$

$R(\Omega) = e^{-i\alpha J_z} e^{-i\beta J_y} e^{-i\gamma J_z}$  is the rotation operator which rotates the system through the three Euler angles  $\Omega = (\alpha, \beta, \gamma)$ , and  $D_{MK}^L$  is a Wigner  $D$ -function.

In Figures 5–7 we plot the projected energy surfaces corresponding to the three different dynamical symmetry limits  $SU(3)$ ,  $SU^*(3)$  and  $O(6)$  of the IVBM.

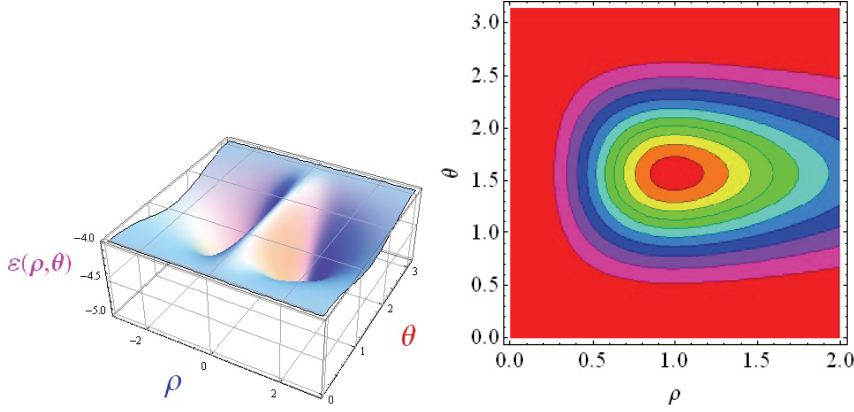


Figure 5. (Color online) Projected energy surface  $\varepsilon(\rho, \theta) = E_{pr}(N; \rho, \theta)/kN$  as 3-dimensional and contour plots corresponding to the Hamiltonian (13) of the  $SU(3)$  limit. For the contour plot only the region  $\rho > 0$  is depicted.

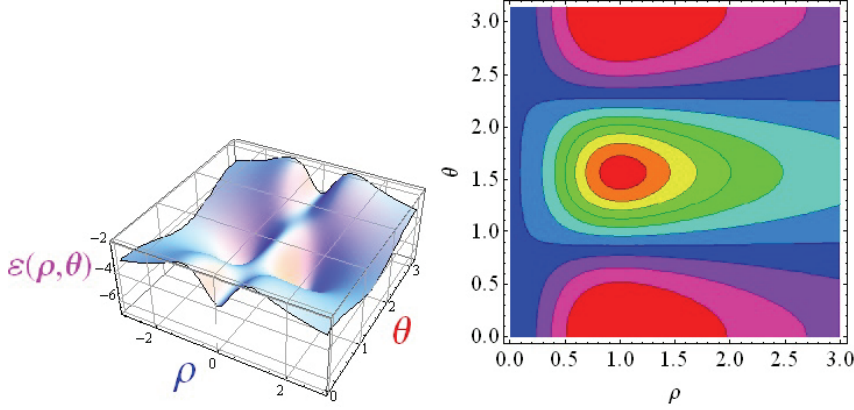


Figure 6. Projected energy surface  $\varepsilon(\rho, \theta) = E_{pr}(N; \rho, \theta)/k'N$  as 3-dimensional and contour plots corresponding to the Hamiltonian (19) of the  $SU^*(3)$  limit. For the contour plot only the region  $\rho > 0$  is depicted.

From Figures 5-6 we see that the angular momentum projection changes the topology of the corresponding potential energy surfaces in both  $SU(3)$  and  $SU^*(3)$  limits. In both dynamical symmetries we see clearly separated minima at  $\rho_0 \simeq 0.9 - 1.1$  and  $\theta_0 \simeq 90^\circ$ . Actually, the minima are obtained at  $\rho_0 = 1$  and  $\theta_0 = 90^\circ$ . In the  $SU(3)$  limit this corresponds to  $\gamma_{eff} = 60^\circ$  (an oblate shape), whereas for the  $SU^*(3)$  one obtains  $\gamma_{eff} = 30^\circ$  corresponding to the case of maximum triaxiality. As can be also seen the obtained minima are slightly unstable with respect to  $\rho$ .

Finally, we consider the projected energy surface in the  $O(6)$  limit, shown in



## Nuclear Shapes in the IVBM

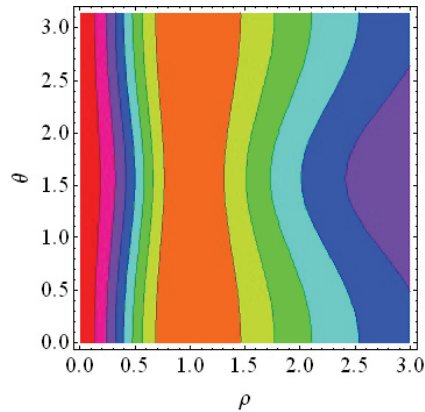


Figure 7. A contour plot of the projected energy surface  $\varepsilon(\rho, \theta)$  in the  $O(6)$  limit. Only the region  $\rho > 0$  is depicted.

Figure 7. We see that although the minimum is at  $\rho_0 = 1$ , the angular momentum projection slightly disturb the typical  $\theta$ -unstable energy surface of this limit.

## 6 Conclusions

In the present paper the possible nuclear shapes are investigated within the framework of the two-fluid Interacting Vector Boson Model. The latter possesses a rich algebraic structure of physically interesting subgroups that define its distinct exactly solvable dynamical limits. Their classical images are obtained by means of the coherent state method using a variation without and with angular momentum projection. The results obtained show that the angular momentum projection turns out to be crucial for obtaining stable triaxial shapes within the framework of the IVBM in its  $SU^*(3)$  limit without breaking the exact dynamical symmetry.

## Acknowledgments

This work was partially supported by the Bulgarian National Foundation for scientific research under Grant Number DID-02/16/17.12.2009.

## References

- [1] P. Cejnar and J. Jolie, *Progr. Part. Nucl. Phys.* **62** (2009) 210.
- [2] F. Iachello, *Phys. Rev. Lett.* **85** (2000) 3580.
- [3] F. Iachello and A. Arima, *The Interacting Boson Model* (Cambridge University Press, Cambridge, 1987).
- [4] F. Iachello and R.D. Levine, *Algebraic Theory of Molecules* (Oxford: Oxford University Press, 1995).

H. G. Ganev

- [5] S. Kuyucak, *Chem. Phys. Lett.* **301** (1999) 435; F. Pérez-Bernal, L.F. Santos, P.H. Vaccaro, and F. Iachello, *Chem. Phys. Lett.* **414** (2005) 398.
- [6] H. Yépez-Martínez, J. Cseh, and P.O. Hess, *Phys. Rev. C* **74** (2006) 024319.
- [7] A. Georgieva, P. Raychev, and R. Roussev, *J. Phys. G* **8** (1982) 1377.
- [8] H.G. Ganev, *Phys. Rev. C* **83** (2011) 034307.
- [9] H.G. Ganev, *Phys. Rev. C* **84** (2011) 054318.
- [10] V. Bargmann and M. Moshynsky, *Nucl. Phys.* **18** (1960) 697.
- [11] V. Bargmann and M. Moshynsky, *Nucl. Phys.* **23** (1961) 177.
- [12] A.I. Georgieva, H.G. Ganev, J.P. Draayer, V.P. Garistov, *Phys. Part. Nucl.* **40** (2009) 461.
- [13] A. Bohr and B.R. Mottelson, *Nuclear Structure*, Vol. II. (W.A. Benjamin Inc., New York, 1975).
- [14] K. Heyde, P. Van Isacker, M. Waroquier, and J. Moreau, *Phys. Rev. C* **29** (1984) 1420.
- [15] G. Thiamova, *Eur. J. Phys. A* **45** (2010) 81.
- [16] S. Kuyucak and I. Morrison, *Phys. Lett. B* **255** (1991) 305.
- [17] P. Van Isacker, A. Bouldjedri, and S. Zerguine, *Nucl. Phys. A* **836** (2010) 225.
- [18] A.E.L. Dieperink, *Nucl. Phys. A* **421** (1984) 189c.
- [19] M.A. Caprio and F. Iachello, *Phys. Rev. Lett.* **93** (2004) 242502.
- [20] J.M. Arias, J.E. Garcia-Ramos, and J. Dukelsky, *Phys. Rev. Lett.* **93** (2004) 212501.
- [21] H.A. Lamme and E. Boeker, *Nucl. Phys. A* **111** (1968) 492.
- [22] P. Ring and P. Shuck, *The Nuclear Many Body Problem* (Springer, 2005).
- [23] D.M. Brink and G.R. Satchler, *Angular Momentum* (Oxford University Press, Oxford, 1968).